Univerza v Ljubljani
Fakulteta za matematiko in fiziko
Oddelek za fiziko
Smer: naravoslovna fizika

BARCHAN DUNES

Seminar 2

Author: Barbara Horvat
Mentor: prof.dr.Rudolf Podgornik

Abstract

Sand dunes occur throughout the world, from coastal and lakeshore plains to arid desert regions. Not just on Earth but also on Mars, Venus etc. In this seminar I am going to talk about barchan dunes: about their creation, movement and shape.

1 Dunes

Def. A sand dune is a hill made by the wind on the coast or in a desert or by the water under the water.

With regard to the wind direction we know two types of dunes:

- longitudinal dunes also called Seif dunes, elongate parallel to the prevailing wind, possibly caused by a larger dune having its smaller sides blown away. They are sharp-crested and range up to 300m in height and 300km in length.
- transverse dunes which are horizontal to the prevailing wind, probably caused by a steady buildup of sand on an already existing minuscule mound. They appear in regions of mainly unidirectional wind and high sand availability.

On the other hand we know also different shapes that were made under different wind conditions so to speak under different wind directions:

- Crescentic

  the most common dune form on Earth (and on Mars) is the crescentic. Crescent-shaped mounds generally are wider than long. The slipface is on the dune's concave side. These dunes form under winds that blow from one direction, and they also are known as barchans, or transverse dunes. Some types of crescentic dunes move faster over desert surfaces than any other type of dune.

- Linear

  straight or slightly sinuous sand ridges typically much longer than they are wide are known as linear dunes. They may be more than 160km long. Linear dunes may occur as isolated ridges, but they generally form sets of parallel ridges separated by miles of sand, gravel, or rocky interdune corridors. Some linear dunes merge to form Y-shaped compound dunes. Many form in bidirectional wind regimes. The long axes of these dunes extend in the resultant direction of sand movement.

- Star

  radially symmetrical, star dunes are pyramidal sand mounds with slipfaces on three or more arms that radiate from the high center of the mound. They tend to accumulate in areas with multidirectional wind regimes. Star dunes grow upward rather than laterally.

- Dome

  oval or circular mounds that generally lack a slipface, dome dunes are rare and occur at the far upwind margins of sand seas.

- Parabolic

  U-shaped mounds of sand with convex noses trailed by elongated arms are parabolic dunes. Sometimes these dunes are called U-shaped, blowout, or hairpin dunes, and they are well known in coastal deserts. Unlike crescentic dunes, their crests point upwind. The elongated arms of parabolic dunes follow rather than lead because they have been fixed by vegetation, while the bulk of the sand in the dune migrates forward.

- Combined types

  occurring wherever winds periodically reverse direction, reversing dunes are varieties of any of the above types. These dunes typically have major and minor slipfaces oriented in opposite directions.

All these dune shapes may occur in three forms:

- simple
  Simple dunes are basic forms with a minimum number of slipfaces that define the geometric type.

- compound
  Compound dunes are large dunes on which smaller dunes of similar shape and slipface orientation are superimposed.
- complex
  Complex dunes are combinations of two or more dune shapes.

Simple dunes represent a wind regime that has not changed in intensity or direction since the formation of the dune, while compound and complex dunes suggest that the intensity and direction of the wind has changed.

2 Barchan dunes

Barchans dunes or barchans (**barkhan** [turkm.], crescent shape dune.) I'm going to talk about mostly are aeolian sand dunes that form in arid regions where unidirectional winds blow on a firm ground with limited sand supply. They propagate along the main wind direction and have a particular shape shown in Figure (1).

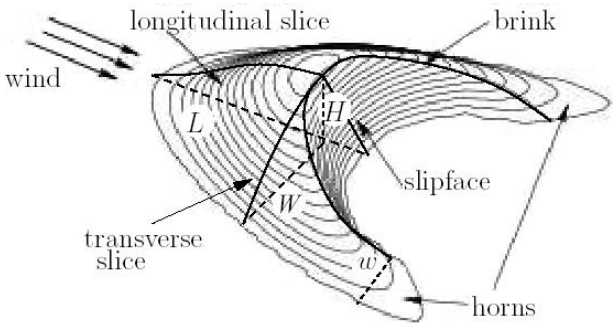

Figure 1: Barchans are crescent-shaped sand dunes formed in arid regions under almost unidirectional wind. On this sketch can be seen all important terminology.

This shape strongly depends on wind's direction: if windblown sand comes from one prevailing direction, a dune will be a crescent-shaped barchan but if winds switch direction seasonally (coming from the southwest for half the year and from the southeast for the other half) a dune will be linear or even worse if wind direction is erratic, a dune may be star-shaped so there would be no barchan. Therefore the wind has to be more than less unidirectional.

We know two types of barchans: aeolian (made by the wind) and subaqueous (made under the water).

Aeolian sand dunes have been analyzed for decades. Main problem here is that experiments take too much time comparing to the amount of results we get from them. On the other hand subaqueous barchan dunes that were recently found have great advantages comparing to aeolian barchans exactly in this manner (see table 1).

barchans	lengthscale	timescale	successful experiments done
aeolian	large	large	just observations in the field
subaqueous	small	small	also experiments in the laboratory

Table 1: The comparison between two types of barchan dunes: made under interaction sand-wind and those made under interaction sand-water. Lengthscale represents dimensions of barchans; timescale time needed for experiment to be done (depends on the speed of a barchan moving across the firm soil). Conclusion we can make is that barchan made under water are much easier to be studied.

3 Sand movement

3.1 Introduction

Aeolian processes or better erosion, deposition and transport of sand caused by the flow of air over the firm soil are mainly responsible for transporting sediments over the surface in arid areas or to be more specific for creation and movement of barchans.

Particles are transported by winds through suspension, saltation (bouncing) and creep (rolling). These processes occur in this order with increasing grain size as can be seen on Figure 2.

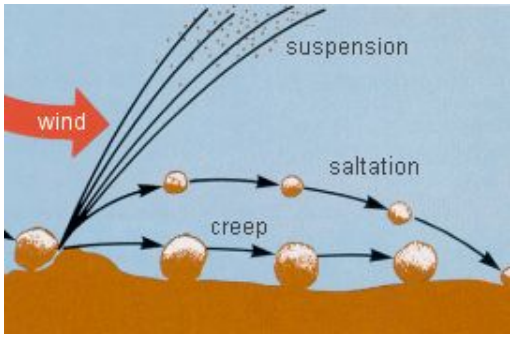

Figure 2: Sand transport.

Small particles may be held in the atmosphere in suspension. Upward currents of air support the weight of suspended particles and hold them indefinitely in the surrounding air. Typical winds near Earth's surface suspend particles less than 0.2 millimeters in diameter and scatter them aloft as dust or haze.
If typical sand storm is considered or better if shear velocity ranges from 0.18-0.6m/s, particles of maximum diameter of 0.04-0.06mm can be transported in suspension. The grains of typical sand dune have a diameter of the order of 0.25mm (see Figure 3) and are therefore transported via bed-load (saltation, creep). This is the reason why transport via suspension will be from now on neglected.

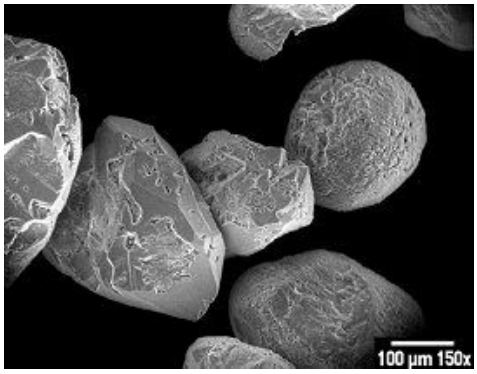

Figure 3: Typical grains in sand dune.

Saltation is downwind movement of particles in a series of jumps or skips. Saltation normally lifts sand-size particles no more than one centimeter above the ground, and proceeds at one-half to one-third the speed of the wind. A saltating grain may hit other grains that jump up to continue the saltation. The grain may also hit larger grains that are too heavy to hop, but that slowly creep forward as they are pushed by saltating grains. Surface creep accounts for as much as 25 percent of grain movement in a desert.
Under the right wind conditions, saltation can become a self-sustaining system of jumping sand grains moving along a dune, clearly visible as swaying patterns of sand about ankle height moving upward toward the dune's crest.

Wind erodes Earth's surface by deflation, the removal of loose, fine-grained particles by the turbulent eddy action of the wind, and by abrasion, the wearing down of surfaces by the grinding action and sand blasting of windborne particles.

Wind-deposited materials hold clues to past as well as to present wind directions and intensities. These features help us understand the forces that molded it. Wind-deposited sand bodies occur as sand sheets, ripples, and dunes (see Figure 4).

Figure 4: On the left side near the big heap where the area is flat you can see sand sheets. The big heap represents dune and the series of small ridges and troughs on the dune are called ripples.

Sand sheets are flat, gently undulating sandy plots of sand surfaced by grains that may be too large for saltation. They form approximately 40 percent of eolian depositional surfaces.

Wind blowing on a sand surface ripples the surface into crests and troughs whose long axes are perpendicular to the wind direction. The average length of jumps during saltation corresponds to the wavelength, or distance between adjacent crests, of the ripples. In ripples, the coarsest materials collect at the crests. This distinguishes small ripples from dunes, where the coarsest materials are generally in the troughs.

Wind-blown sand moves up the gentle upwind side of the dune by saltation or creep. Sand accumulates at the brink, the top of the slipface. When the buildup of sand at the brink exceeds the angle of repose (about 34°), a small avalanche of grains slides down the slipface. Grain by grain, the dune moves downwind.

Accumulations of sediment blown by the wind into a mound or ridge, dunes have gentle upwind slopes on the wind-facing side. The downwind portion of the dune, the lee slope, is commonly a steep avalanche slope referred to as a slipface (see Figure 1). Dunes may have more than one slipface. The minimum height of a slipface is about 30 centimeters.

3.2 A continuum saltation model

There were several attempts to describe sand movement or so to speak flux (see Figure 5).

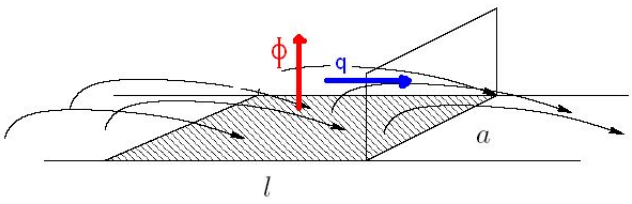

Figure 5: The flux q is the volume of sand which crosses a unit line transverse to the wind per unit time. If the typical path of a grain has a hop length l, the incident flux of grains ϕ, which is the volume of grains colliding a unit area per unit time, is equal to q/l.

The simplest law was proposed by Bagnold, a bit more complicated by Lettau and Lettau (see comparison of saturated sand fluxes), there was made a huge amount of measurements, numerical simulations on a grain scale etc. However, whether the problem appeared at the windward foot of an isolated dune, where the bed changes from bedrock to sand, or when trying to calculate the evolution of macroscopic geomorphologies from models that base on a grain scale. So there had to be made a new model: a continuum saltation model. This model represents bed load is as a thin fluid on top of immobile sand bed and neglects lateral transport (caused by gravity, diffusion) due to restriction to a two dimensional description.

There are three phenomenological parameters of the model to be considered: a reference height for the grain-air interaction (z_1), an effective restitution coefficient for the grain-bed interaction (α), and a multiplication factor characterizing the chain reaction caused by the impacts leading to a typical time or length scale of the saturation transients (γ).

Closed model[1] derivated from the mass and momentum conservation in presence of erosion and external forces yields:

$$\frac{\partial \rho}{t} + \frac{\partial}{\partial x}(\rho u) = \frac{1}{t_s}\rho(1 - \frac{\rho}{\rho_s}) + \Gamma_a \tag{1}$$

$$\rho_s = \frac{2\alpha}{g}(\tau - \tau_t) \tag{2}$$

$$t_s = \frac{2\alpha u}{g}\frac{\tau_t}{\gamma(\tau - \tau_t)} \tag{3}$$

$$\frac{\partial u}{\partial t} + (u\frac{\partial}{\partial x})u = \frac{3}{4}C_d\frac{\rho_{air}}{\rho_{qartz}}\frac{1}{d}(v_{eff} - u)|v_{eff} - u| - \frac{g}{2\alpha} \tag{4}$$

$$v_{eff} = \frac{u_*}{\kappa}\sqrt{1 - \frac{\tau_{g0}}{\tau}}(2A_1 - 2 + \ln\frac{z_1}{z_0}), \qquad z_0 < z_1 << z_m \tag{5}$$

Here are:

u	sand velocity in the saltation layer	A_1	$\sqrt{1 + \frac{z_1}{z_m}\frac{\tau_{g0}}{\tau - \tau_{g0}}}$
u_*	shear velocity	Γ_a	aerodynamics entrainment
v_{eff}	effective wind velocity	κ	~ 0.4 von Kármán constant
ρ	sand density in the saltation layer	C_d	dragg coefficient
ρ_s	saturated sand density	d	grain diameter
ρ_{air}	air density	g	gravitational acceleration
ρ_{quartz}	grain/quartz density	z_0	roughness
τ	air shear stress	z_1	reference height
τ_t	threshold	z_m	mean saltation height
τ_{g0}	grain born shear stress at the ground	x	along the wind direction
t_s	characteristic/saturation time		

Table 2: Definition of main quantities.

The coupled differential equations (1 and 4) for the average density and velocity of sand in the saltation layer reproduce two equilibrium relations for the sand flux and the time evolution of the sand flux as predicted by microscopic saltation models (we neglected aerodynamics entrainment):

- saturated flux

  When analytically calculating stationary solution ($\frac{\partial}{\partial t} = 0$) from equations 1 and 4, considering a constant external shear stress ($\tau(x,t) = \tau$) and a homogeneous bed ($\frac{\partial}{\partial x} = 0$), we obtain for:

  1. shear velocities below the threshold ($u_* < u_{*t}$):
     $\rho_s(u_*) = 0$, $u_s(u_*) = 0$, $q_s(u_*) = 0$

[1] for derivation see [17]

2. above the threshold ($u_* > u_{*t}$):
   $\rho_s(u_*) = \frac{2\alpha\rho_{air}}{g}(u_*^2 - u_{*t}^2)$

$$u_s(u_*) = \frac{2u_*}{\kappa}\sqrt{\frac{z_1}{z_m} + (1 - \frac{z_1}{z_m})\frac{u_{*t}^2}{u_*^2}} - \frac{2u_{*t}}{\kappa} + u_{st}\ , \quad where \tag{6}$$

   $u_{st} \equiv u_s(u_{*t}) = \frac{u_{*t}}{\kappa}\ln\frac{z_1}{z_0} - \sqrt{\frac{2gd\rho_{quartz}}{3\alpha C_d\rho_{air}}}$ represents minimum velocity of the grains in the saltation layer occurring at the threshold

$$q_s(u_*) = u_s\rho_s = \frac{2\alpha\rho_{air}}{g}(u_*^2 - u_{*t}^2)(\frac{2u_*}{\kappa}\sqrt{\frac{z_1}{z_m} + (1 - \frac{z_1}{z_m})\frac{u_{*t}^2}{u_*^2}} - \frac{2u_{*t}}{\kappa} + u_{st}) \tag{7}$$

By fitting saturated flux (equation 7) to measured data α and z_1 are determined. For comparison of this flux (q_S) with Bagnold's ($q_B = C_B\frac{\rho_{air}}{g}\sqrt{\frac{d}{D}}u_*^3$), Lettau and Lettau's ($q_L = C_L\frac{\rho_{air}}{g}u_*^2(u_* - u_{*t})$), Sørensen's ($q_{S\emptyset} = C_{S\emptyset}\frac{\rho_{air}}{g}u_*(u_* - u_{*t})(u_* + 7.6 \cdot u_{*t} + 205)$) and wind tunnel data where was taken $g = 9.81m/s^2$, $\rho_{air} = 1.225kg/m^3$, $\rho_{quartz} = 2650kg/m^3$, $z_m = 0.04m$, $z_0 = 2.5 \cdot 10^{-5}$, $D = d = 250\mu m$ (D represents standard grain diameter), $C_d = 3$ and $u_{*t} = 0.28m/s$ from which it was obtained $\alpha = 0.35$, $z_1 = 0.005m$, $C_B = 1.98$, $C_L 4.10$ and $C_{S\emptyset} = 0.011$ see Figure 6.

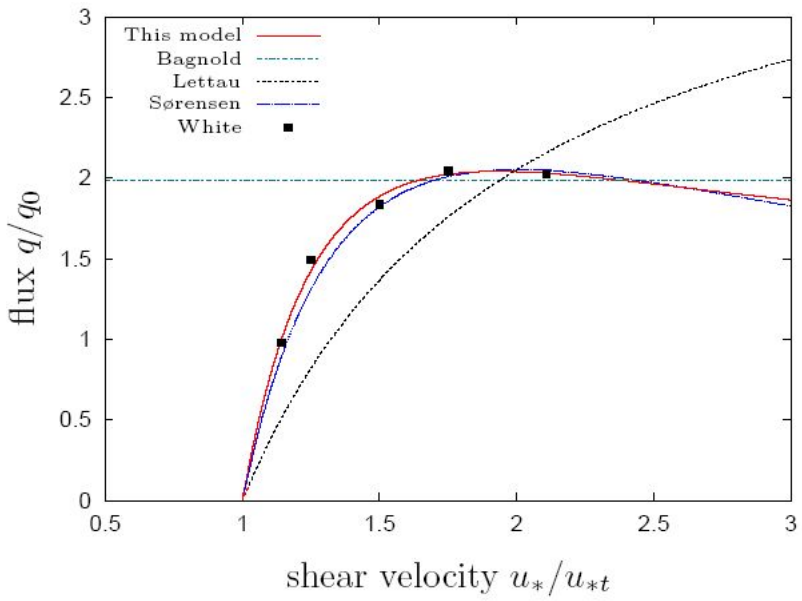

Figure 6: Comparison of different theoretical fluxes fitted to measurements presented by dots. All fluxes are normalize by $q_0 = \rho_{air}/(gu_*^3)$. As can be seen all laws show more then less a cubic dependence on the shear velocity when it is high.

- time evolution of the sand flux

  The time evolution of the topography h(x,t) is given by mass conservation (when we neglect the perturbations of the wind field caused by the topography and take into consideration just the sand transport):

$$\frac{\partial h}{\partial t} = -\frac{1}{\rho_{sand}}\frac{\partial q}{\partial x}, \quad where \tag{8}$$

  ρ_{sand} presents mean density of the immobile dune sand. To obtain the sand flux q(x,t) equations 1 and 4 have to be solved. On the other hand we can simplify this model by using the stationary solution in equations 1, 4 (time scale of the surface evolution is several orders of magnitude larger than the time scale of saltation), with taking into consideration convective term ($u\partial_x u$) that is only important

at places where large velocity gradients occur (outside the wake regions (which are behind the brink) it can be neglected), that near the threshold τ_t $v_{eff}(\rho)$ can be approximated by $v_{eff}(\rho_s)$ (ρ can be replaced by ρ_s; u is decoupled from the ρ) so equation 6 can be inserted in equation 1 which rewritten yields:

$$\frac{\partial}{\partial x}q = \frac{1}{l_s}q_s(1 - \frac{q}{q_s}), \quad where \tag{9}$$

$q = \rho u_s$, $q_s = \rho_s u_s$, $l_s = \frac{2\alpha}{\gamma}\frac{u_s^2}{g}\frac{\tau_t}{\tau - \tau_t}$ (saturation length); (equation 9 is known as the charge equation).

3.3 Minimal model

Minimal model, which is used for calculating the shape and time evolution of the dune, can be thought of as four (almost) independent parts: the stationary wind field over a complex terrain, the stationary aeolian sand transport, the time evolution of the surface due to erosion and avalanches.

Let τ_0 be the wind shear stress over a flat surface (it is scale invariant) and $\hat{\tau}(x)$ a non-local perturbation of the undisturbed τ_0 due to the perturbation of ground h(x) (dune isn't a flat object). According to the perturbation theory we can write the air shear stress:

$$\tau(x) = \tau_0(1 + \hat{\tau}(x)), \quad where \tag{10}$$

$$\hat{\tau}(x) = A(\frac{1}{\pi}\int_{-\infty}^{\infty}\frac{h'}{x - \xi}d\xi + Bh'), \quad where \tag{11}$$

h' denotes the spatial derivate of the dune's profile h(x) in the wind direction, A controls the pressure effect, where the whole shape acts on the wind flow, B controls the destabilizing effect, which ensures that the maximum speed of the flow is reached before the dune summit. Here are A and B logarithmically depend on the ratio between the characteristic length L of the dune and the roughness length z_0 of the surface. We have to denote that $\hat{\tau} \propto \frac{H}{L}$ and that Bh' represents symmetry breaking contribution (comes from the non-linear convection term in the stationary Navier-Stokes equation). In terms of perturbation theory has to be $H/L \sim 0.3$. That is always true on the windward side. However, flow separation occurs at the brink, which is out of the scope of perturbation theory. They found a solution: a separation bubble that comprises the recirculation flow, which reaches from the brink (detachment point) to the bottom (reattachment point) - see Figure 7.

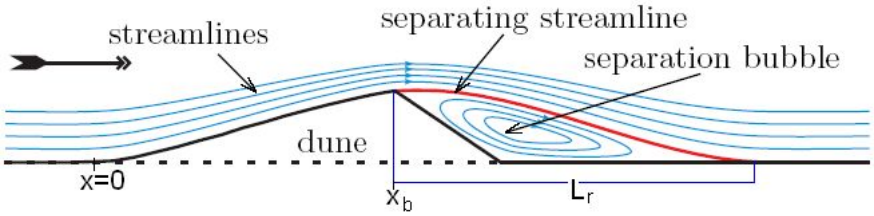

Figure 7: Sketch of a central slice of a barchan and the separation bubble.

Separating streamline is modeled by a third order polynomial that is a smooth continuation of the profile h(x) at the brink x_b at the reattachment point $x_b + L_r$. So requirements are: $h(x_b) = s(0)$, $h'(x_b) = s'(0)$, $s(L_r) = 0$, $= s'(L_r) = 0$, where s defines streamline.

Minimal model includes also a continuum saltation model which comes in with the charge equation 9. A spatial change in the sand flux causes erosion/deposition and leads to a change in the shape. The time evolution of the surface can be calculated from the conservation of mass:

$$\frac{\partial h}{\partial t} = -\frac{1}{\rho_{sand}}\frac{\partial q}{\partial x}, \tag{12}$$

which is the only remaining time equation.

So the solution of this model yields:

An initial surface h is used to start the time evolution. If flow separation has to be modeled the separating streamline s(x) is calculated. As follows, the air shear stress $\tau(x)$ onto the given surface (h or s) is calculated from equation 10, then from equation 9 the air shear stress, the integration forward in time using equation 12 and finally, sand is eroded and transported downhill if the local angle $\partial_x h$ exceeds the angle of repose (34°). This redistribution of mass (avalanches) is performed until the surface slope has relaxed below the critical angle. The time integration is calculated until the final shape is obtained.

Results obtained using minimal model are shown on Figure 8 (initial heap was Gaussian). It is pretty obvious

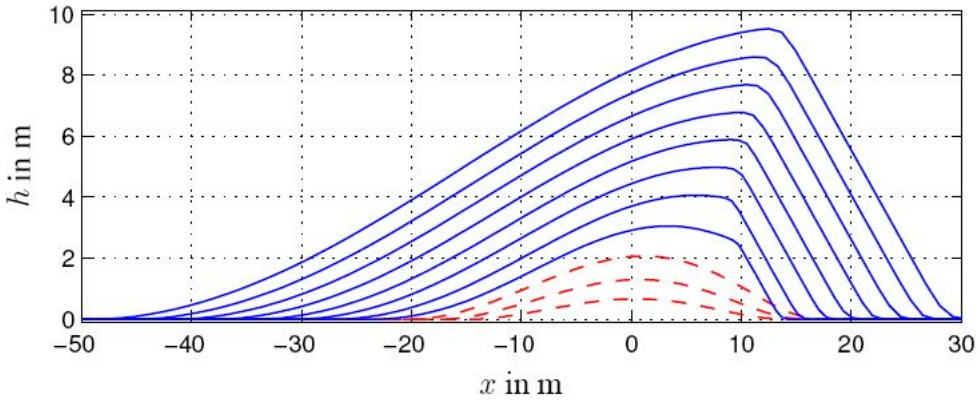

Figure 8: The solution for large masses (blue) are dunes including a slipface (above a critical height), whereas for small masses heaps develop (red).

that shape isn't the same for large and small dunes, there is no scale invariance. The conclusion we can make is that there should exist a typical lengthscale ($=l_s$). Even more, when observing the sizes of dunes we see that there are no barchans below certain height. So there should exist a minimum size of barchan respectively a typical lengthscale ($=l_s$).[2]

3.4 3D C_C^C model

Because of the boundary layer separation along the brink, a large eddy develops downwind and wind speed decreases dramatically. Therefore, the incoming blown sand is dropped close to the brink and this is the reason why barchans are known as very good sand trappers. But on the other hand sand leak was noticed at the tip of the horns, where no recirculation bubble develops. This leads to the conclusion that barchans are three dimensional objects, whose center part and horns have completelly different trapping efficiency (see Figure 9). So there has to exist lateral coupling mechanism. The best candidate is the grain motion; sand transport can be divided into two parts: grains in saltation (the saltons) and grains in reptation (the reptons) - see Figure 10.

Because the lateral wind deflection is weak it is assumed that saltons follow quasi 2D trajectory in a vertical plane (except when they collide with the dune). At each collision they can rebound in many directions

[2]Connection of minimum height with saturation length

Consider the wind blowing over a sand surface. It can dislodge grains and accelerate them until they reach the wind velocity. During this process, a grain covers a distance which scales with $l_{saltation}$ ($= l_{sal}$). When a dragged grain collides back the sand bed it dislodges and pushes new grains, some of them being again accelerated by the wind. So the sand flux increases. After a few times l_{sal} all the grains that can be accelerated by the wind are mobilized and no grain can quit the sand bed without another grain being deposited: the sand flux gets saturated. According to this description, the flux saturation length appears to be proportional to l_{sal}. So the conclusion is: on a dune smaller than the flux saturation length the flux always increases. Therefore the dune can only be eroded. But on the other hand for a larger dune the grain flux becomes oversaturated on the downwind slope and can deposit sand grains. In this way larger dunes survive the erosion by the wind.

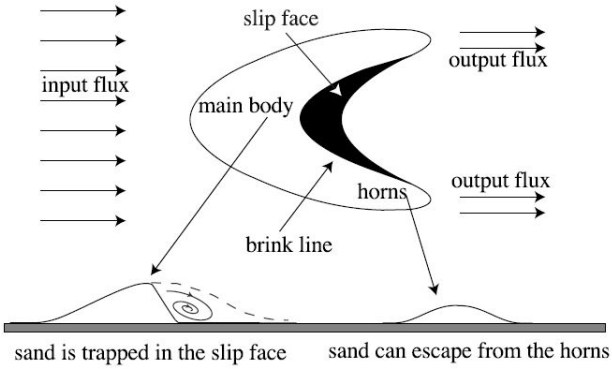

Figure 9: As observed in the field, sand grains can escape from the horns, but not from the main dune body where they are trapped into the slipface. This difference of behaviour between the main body and the horns is crucial for understanding the barchans.

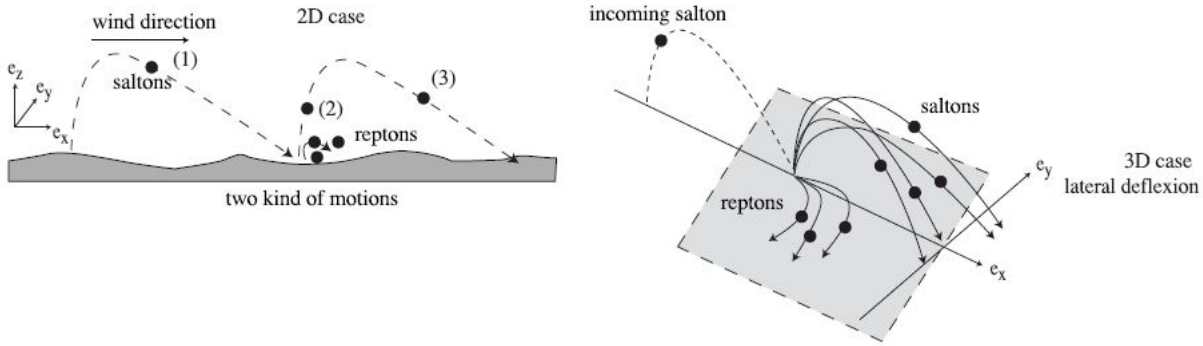

Figure 10: Trajectories of saltons are deflected randomly at each collision, while the reptons are always pushed down along the steepest slope which is due to gravity.

(depends on the local surface properties) which has for the consequence an induced lateral sand flux. It is assumed that in average the deflection of saltons is smaller than for reptons (they are always driven toward the steepest slope) due to the strong dependence of the defledction by collisions on the surface roughness. Therefore, the sand flux deflection due to the saltation collisions is neglected. On the other hand we can't neglect the lateral coupling induced by reptons which roll down the steepest slope due to the gravity.

The part of the flux due to the reptons is assumed to be proportional to the saltation flux (q_{sal}) due to the fact that reptons are created by saltation impacts. So the flux of reptons yields:

$$\vec{q}_{rep} = \alpha q_{sal}(\vec{e}_x - \beta\vec{\nabla}h), \quad where \tag{13}$$

α coefficient represents the fraction of the total sand flux due to reptation on a flat bed. However, if the bed is not flat, the flux is corrected to the first order of the topography h derivates by a coefficient β and directed along the steepest slope to take into account the deflection of reptons trajectories by gravity. The total sand flux should now yield:

$$\vec{q} = q_{sal}(1+\alpha)\vec{e}_x - \alpha\beta q_{sal}\vec{\nabla}h), \quad where \tag{14}$$

assumption that saltation trajectories are 2D is included. According to the assumption that reptation flux instantaneously follows the saltation flux, there is no other charge equation than equation 9 where $q_{sal} = q$. On the other hand equation that describes mass conservation (equation 8) changes:

$$\frac{\partial h}{\partial t} + \frac{\partial q_{sal}}{\partial x} + \vec{\nabla}\vec{q}_{rep} = 0. \tag{15}$$

When inserting $D = \alpha\beta/(1+\alpha)$ and $\tilde{q} = (1+\alpha)q_{sal}$ into equations 9 and 15, we obtain:

$$\frac{\partial \tilde{q}}{\partial x} = \frac{1}{l_s}\tilde{q}_s(1 - \frac{\tilde{q}}{\tilde{q}_s}), \tag{16}$$

$$\frac{\partial h}{\partial t} + \frac{\partial \tilde{q}}{\partial x} = D(\frac{\partial}{\partial x}(\tilde{q}\frac{\partial}{\partial x}h) + \frac{\partial}{\partial y}(\tilde{q}\frac{\partial}{\partial y}h)). \tag{17}$$

Before comparing 3D C_C^C model to the minimal model (2D) I have to mention that also equation 11 doesn't change. So when making a comparison, one can notice that we got one more phenomenological parameter (D) which seems to be connected to the diffusion coefficient. On the other hand avalanches are computed in three dimensions: if the local slope exceeds the threshold μ_d the sand flux is increased by adding an extra avalanche flux:

$$\vec{q_a} = E(\delta\mu)\vec{\nabla}h, \quad where \tag{18}$$

$\delta\mu = 0$ when the slope is lower than μ_d and $\delta\mu = |\vec{\nabla}h|^2 - \mu_d^2$ otherwise.

This model gives us the answer on the formation of the crescentic shape of barchans (which is pretty obvious on Figures 11, 12, 13, 14 and 15).

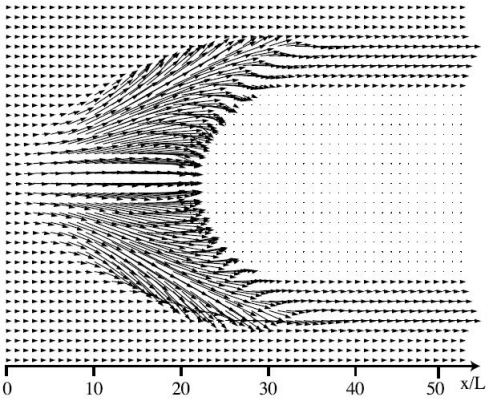

Figure 11: The arrows indicate the direction of the total sand flux on the whole barchan. The deviation towards the horns is clearly visible as the sand captured by the slipface.

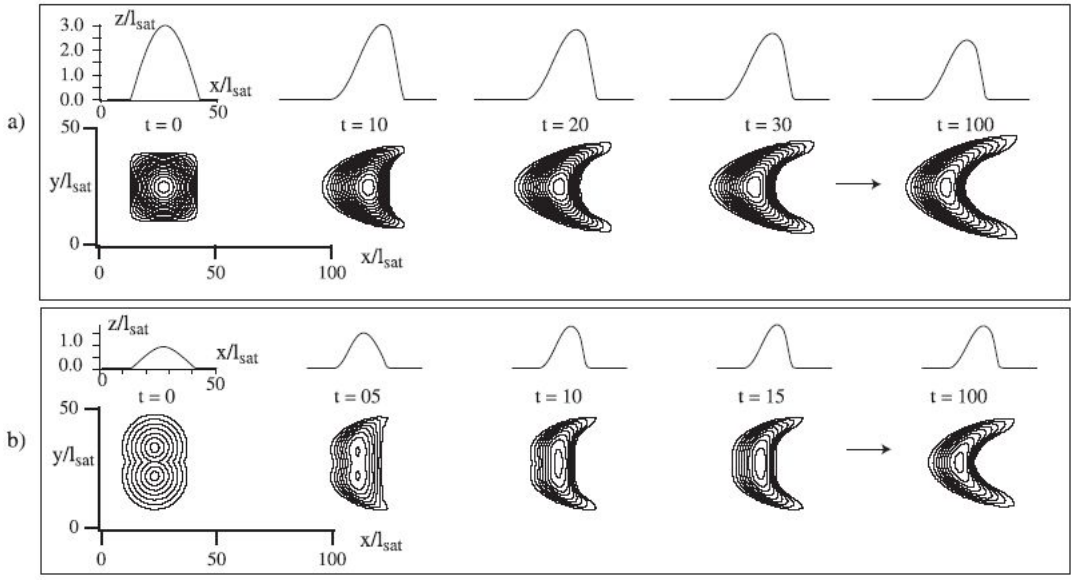

Figure 12: a) Evolution of an initial cosine bump sand pile. In the beginning the horns move faster than the central part of the dune, leading to the formation of the crescentic shape which reaches an equilibrium due to the lateral sand flux which feeds the horns. b) Evolution of a bi-cone sand pile. The part of the flux sensitive to the local slope tends to fill up the gap between both maxima. The whole mass is redistributed and a single barchan shape is obtained. This shows that emergence of a crescentic shape is independent on initial shape.

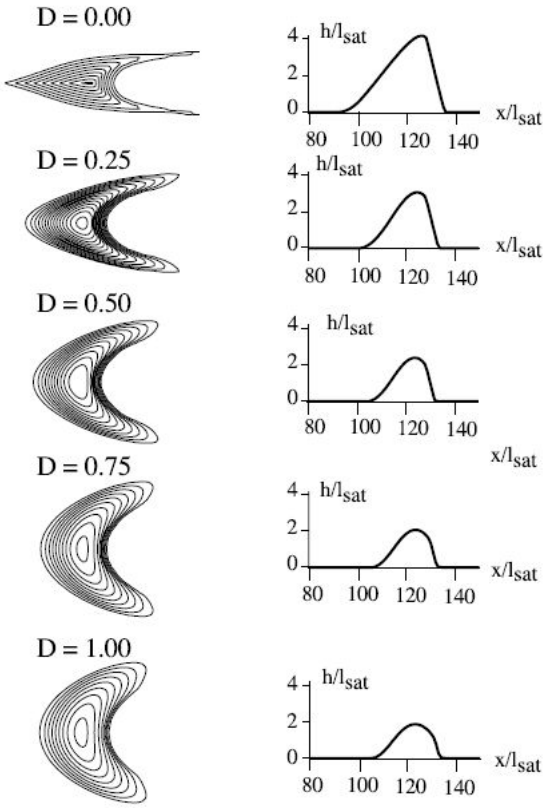

Figure 13: Different 3D shapes obtained for different values of D and for the same initial sand pile. On the right is presented central longitudinal slice. It is obvious that D (conection to the lateral sand flux) has a crucial influence on global morphology.

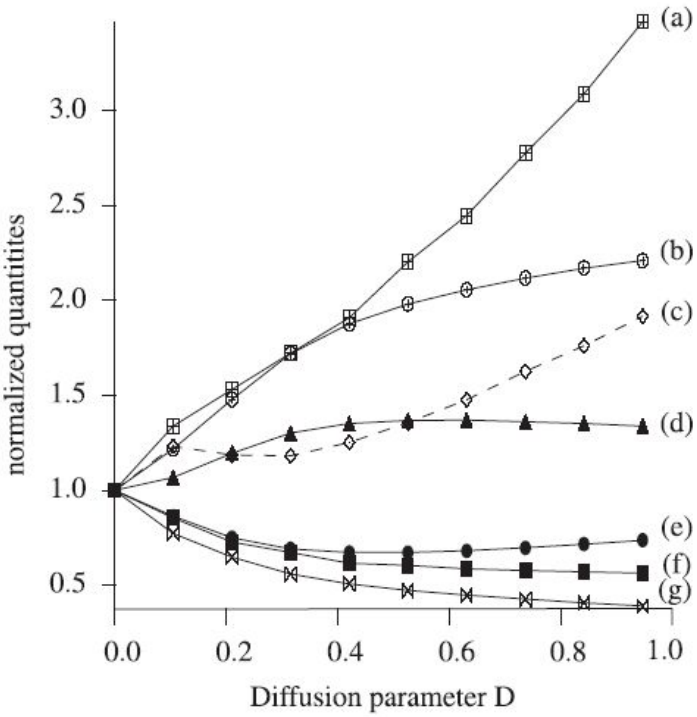

Figure 14: Dependence of barchan's properties on the coupling coefficient D. For a reference is taken D=0. The properties are: (a) width of the horn, (b) total width, (c) equilibrium input flux, (d) speed of the dune, (e) total length (including horns), (f) length of the center slice, (g) maximum height.

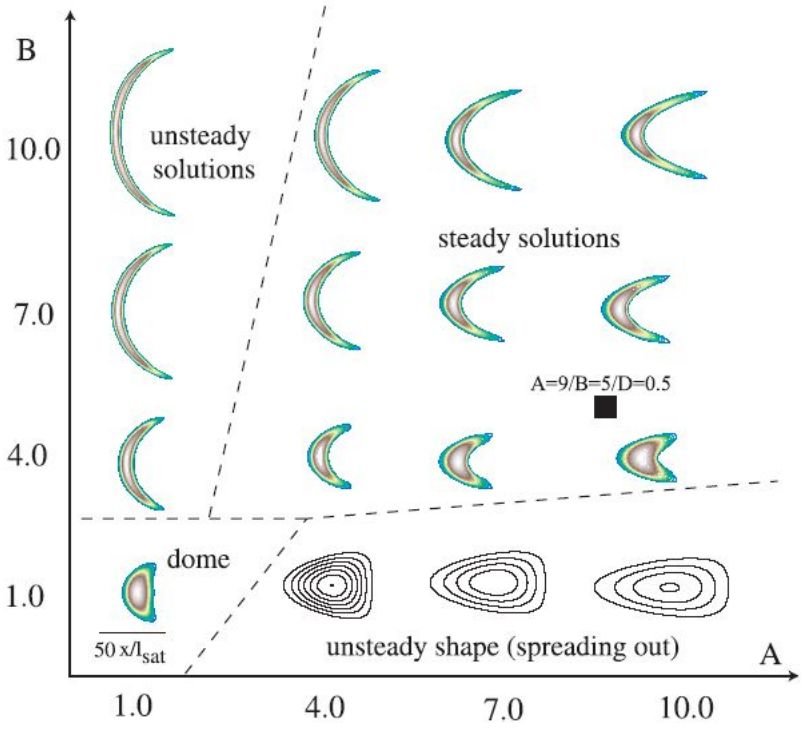

Figure 15: A phase diagram where D is kept constant and parameters A, B are varying. Evolution from a cosine sand pile is observed. The dashed lines separate the different stability and shape domains. It is obvious that A effects curvature (L increases, W decreases), B effects slope (slipface appears, $\partial_x h$ increases, W increases) and D represents lateral coupling (H decreases, W and horns width increase, output flux increases).

4 Experiments and observations

4.1 Field observations

4.1.1 Dunes' morphology

As shown on Figures 16 and 17 there are in first approximation four morphologic parameters by which barchan dune can be described. Those parameters are: the length L, the width W, the height H and the horn length L_{horns}.

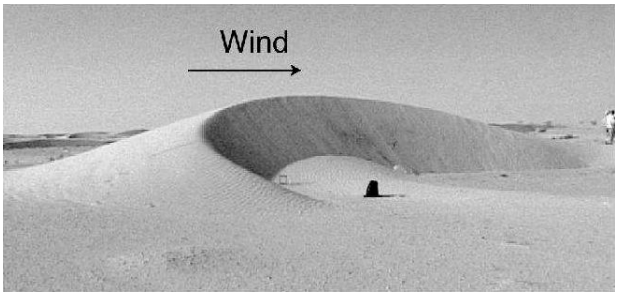

Figure 16: A small barchan ($\simeq$3m high) from Mauritania propagates downwind at one hundred meters per year. From this photo it might not be quite obvious that horns have always different lengths due to the fluctuations of wind direction. So they always have to be measured separately and averaged (L_{horns}).

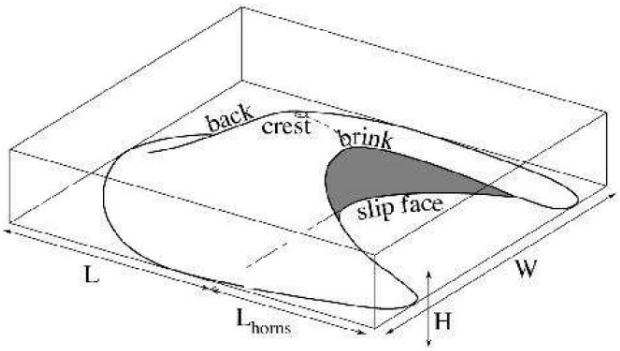

Figure 17: Sketch of a barchan dune with all four morphologic parameters.

Rerlationships got from field measurements are shown on Figures 18, 19.

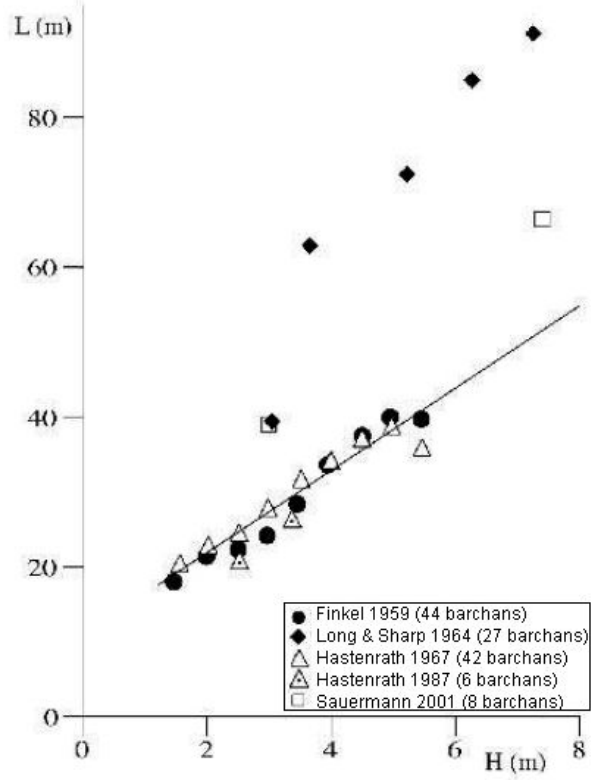

Figure 18: Relationship between the dune length L and height H determined from field measurements averaged by ranges of heights. (For example: barchans between 1m and 2m high were considered, their height, length, width were averaged; that gave one point on this and on the Figures 19, 21, 25 and 26.) The solid line is the best linear fit to the points corresponding to barchans from Peru.

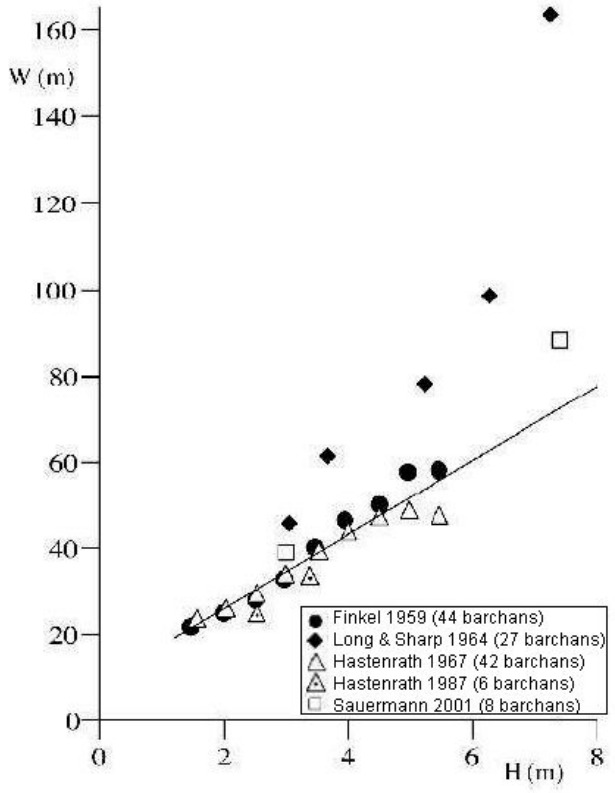

Figure 19: Relationship between barchan width W and height H determined from field measurements averaged by ranges of heights. The solid line is the best linear fit to the points corresponding to barchans from Peru.

Data show large statistical dispersion due to the variations of the control parameters on the field. So there is a dependence of the dune shape on the local conditions: the wind regime, the sand supply, the presence or not of other dunes in the surrounding area, the nature of the soil etc. Despite all that, clear linear relationships between the height H, the length L and the width W were found in the field (just different coefficients):

$$W = W_0 + \rho_W H, \tag{19}$$

$$L = L_0 + \rho_L H. \tag{20}$$

The best linear fits give $\rho_W = 8.6$ and $\rho_L = 5.5$, $L_0 = 10.8m$, $W_0 = 8.8m$. But L, H, W are not proportional: dunes of different heights have different shapes (small dunes present a broad domed convexity around the crest, clearly separated from the brink, while large dunes have the crest straight to the brink as shown on Figure 20). So barchans are not scale invariant objects. According to that, there should exist a typical lengthscale (related to L_0, W_0) in the mechanisms leading to the dune propagation.

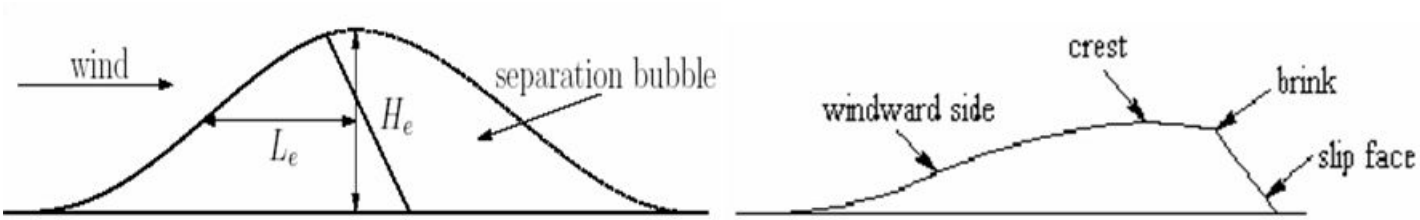

Figure 20: The left sketch represents a large barchan while the right a small one.

From Figures 18 and 19 is also obvious that dunes' morphology depends on the dune field. But it also depends on the wind strength (stronger the wind, smaller the width W, more developed the horns L_{horns}), on the grain size, the density of dunes, the sand supply, the wind direction etc.

Figure 21 shows the relation between mean length of the horns L_{horns} and the height H: $L_{horns} \simeq 9.1H$.

That relation is approximately the same for all the dune fields measured. The conclusion is that the scaling law of the horns length should be simpler than that of the back dimensions.

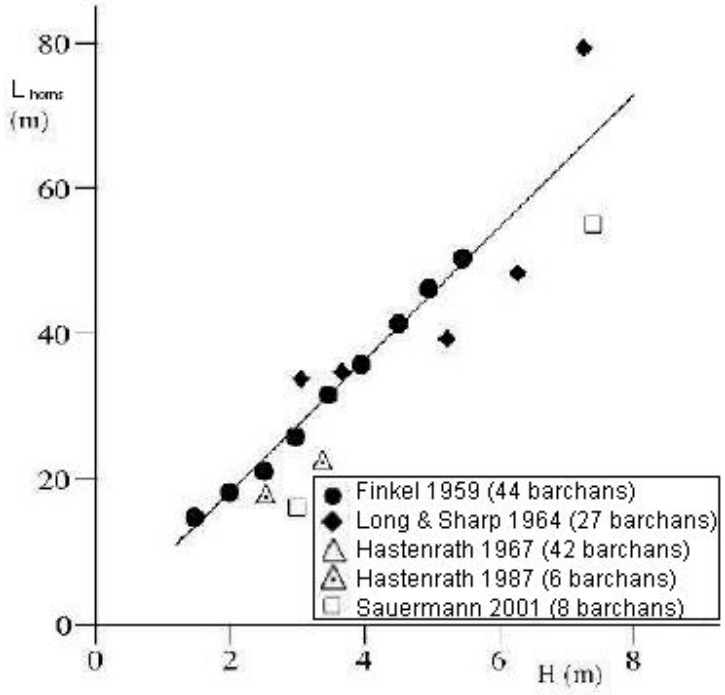

Figure 21: Relationships between the horn length L_{horns} and the height H determined from field measurements averaged by ranges of heights. The solid line is the best linear fit to the points corresponding to barchans from Peru.

4.1.2 Longitudinal profiles

On Figure 22 is shown terminology I am going to use at this point.

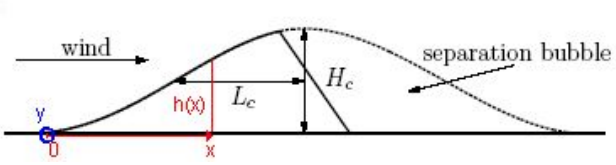

Figure 22: Longitudinal cut along the symmetry plane.

Experimentally got dependence for all windward profiles (when steady-state conditions (influx=outflux) or not) yield:

$$h(x) \approx H_e \cos^{\alpha}(x/L_{\alpha}), \quad where \tag{21}$$

$$L_{\alpha} \equiv L_e / \arccos(2^{-1/\alpha}), \quad with \tag{22}$$

$\alpha \approx 3.0$ for dunes and $\alpha \approx 1.8$ for heaps. This relationship is quite obvious on the insets of Figure 23a) where are also shown steady-state results for the longitudinal profiles for different masses and wind speeds obtained by numerical solution of the minimal model. As you can see all length-height curves can be superimposed on a single curve by rescaling lengths and heights by their values L_c, H_c. Red circled area is the heap area where is obvious that all heaps have more then less the same length: $L_0 \leq L \leq L_c \sim 1.5L_0$ in units l_s^0, and that there is a minimum size for steady-state isolated heaps migrating over plane bedrock. That is even more obvious on Figure 23 b) where $L_0, L_c \propto l_s^0$, $L_0 \approx 0.7L_c$.

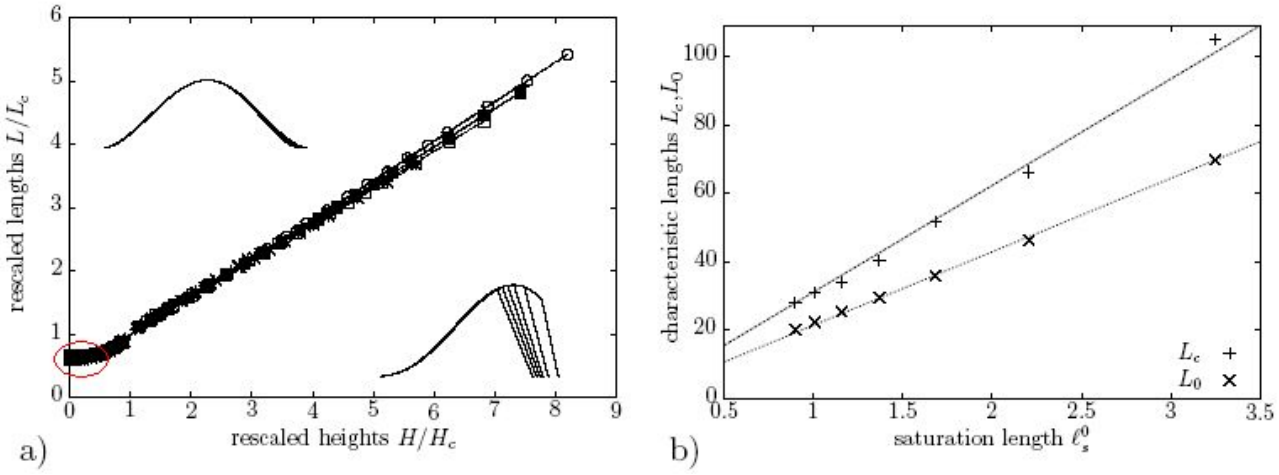

Figure 23: a) Length-height relations of windward longitudinal steady-state profiles for different masses (1-676m^2) and wind speeds ($\frac{\tau^0}{\tau_t} = 1.4, 1.6, 1.8, \ldots, 2.6$). As can be seen all curves collapse onto one curve when heights and lengths are normalized to their values L_c, H_c at the shape transition. The inset shows that windward profile of all dunes are the same and of all heaps are the same (when steady-state condition). b) The transition length L_c and the minimum heap length $L_0 \approx 0.7L_c$ scale linearly with l_s^0.

Here are:

L_0	minimal heap length
L_c	critical/transition length
H_0	minimal heap height
H_c	critical/transition height
l_s^0	$= l_s(\tau^0)$= saturation length over the flat bed
τ^0	reference shear stress over the flat bed

Table 3: Definition of main quantities.

$H_c, \frac{H_c}{L_c}$ depend on the wind strength. These relationships were estimated analytically by taking in concern that the flux over a longitudinal slice has to vanish upon creation of a slipface or: $\frac{H_c}{L_c} \propto 1 - \frac{\tau_t}{\tau^0}$.

4.1.3 Barchans' velocity

When talking about field observations of barchans' propagations we talk about barchans velocity. It is obvious that small dunes move faster than large ones (see Figure 24):

barchans	height	propagating speed
small	3m	15-60m/year
large	15m	4-15m/year

Table 4: The comparison of barchan speed for small and large dunes.

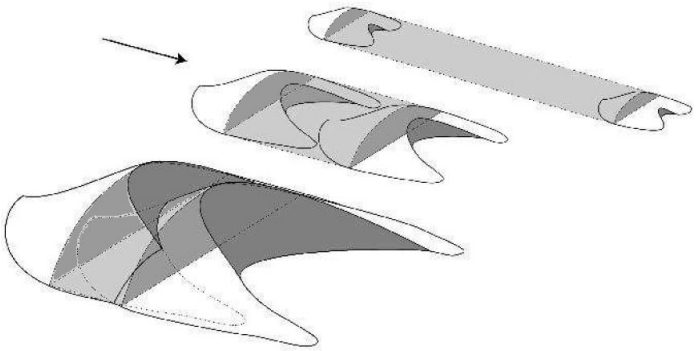

Figure 24: Relation between the dune velocity and its height. On this sketch are three dunes at initial time and after some time t. It is obviously, that smaller dunes are faster and that the area Wct is almost independent of the dune size.

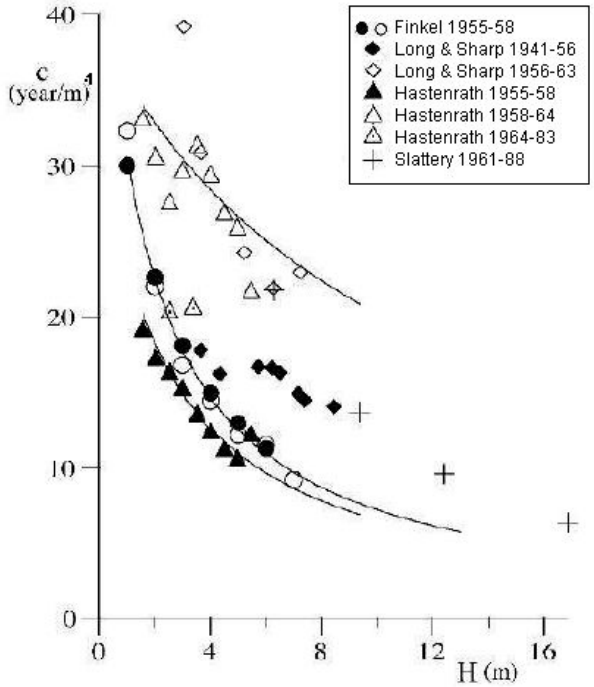

Figure 25: Dune velocity as a function of height. The solid line is the best linear fit to the points corresponding to barchans from Peru. Fit is of the form $c \simeq \frac{Q}{H_0+H}$.

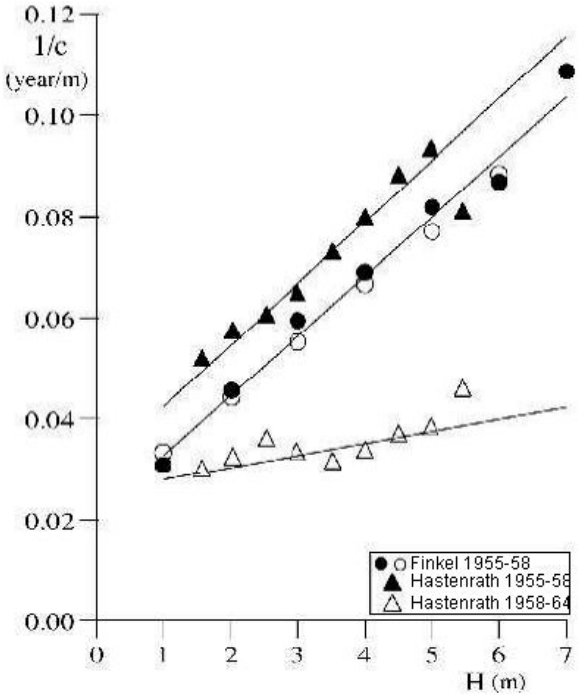

Figure 26: Inverse dune velocity as a function of height. The solid line is the best linear fit to the points corresponding to barchans from Peru.

Figure 25 shows dune velocity as a function of height, Figure 26 dependence of inverse dune velocity of height. Barchan velocity c is different for different places and depends on time because of dependence on fluctuating parameters (wind speed, sand supply). Nonetheless, the relationship between velocity and height yields:

$$c \simeq \frac{Q}{(H_0 + H)} \tag{23}$$

(shown on Figure 26) where $Q \simeq 85 - 425 m^2/year$ (depends on year when measured), $H_0 \simeq 1.8 - 10.9 m$ (depends on year when measured). So the time needed for dune to travel over its own length is:

$$T_{turnover} = \frac{L}{c} \simeq \frac{L(H_0 + H)}{Q}. \tag{24}$$

On the other hand is this time also the typical period of the cycle of motion of a grain of the dune.

barchans	height	$T_{turnover}$
small	3m	5months-2years
large	15m	6-25years

Table 5: The comparison of barchan period of the cycle of motion for small and large dunes.

4.1.4 Barchans as solitons

Field evidence and also underwater experiments show that two dunes are able to pass through one another while still preserving their shape. The crucial parameters for this solitary-wave behaviour are the heights of the two colliding dunes (let the height of the bigger dune be H and the smaller one h). When smaller barchan bumps into the larger one that leads to a hybrid state in which the two dunes are fused in a complex pattern. Three different situations can be observed: coalescence, breeding and solitary-wave behaviour, depending on the relative sizes of the two dunes. The stability of the slip face of the upwind dune crucially influences the final state of the dunes leaving the hybrid state, as well as their relative velocities. When $\Delta H/h$ is small ($\Delta H = H - h$), the dunes move with similar velocities and solitary-wave behaviour occurs (see Figure 27).

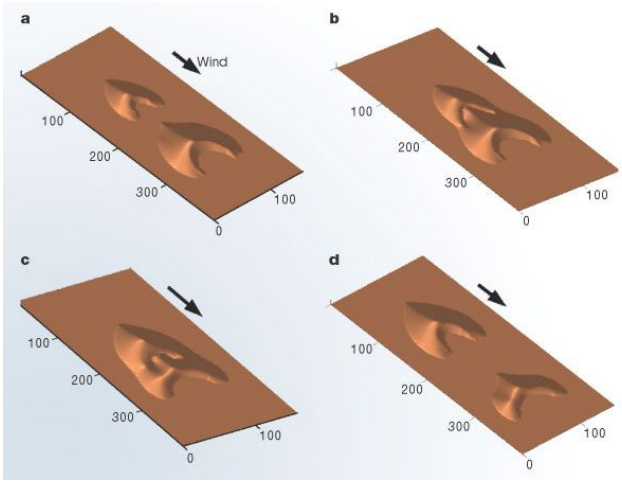

Figure 27: Time series of the solitary-wave behaviour of two barchan sand dunes placed one in front of the other. Parameters are H=7.5m and H/h=0.9; distances are in meters. a) The dunes in their characteristic forms; b) 0.48 years after a, the smaller dune bumps into the larger one; c) hybrid state 0.63 years after a; d) the two dunes depart from the hybrid state (1.42 years after a).

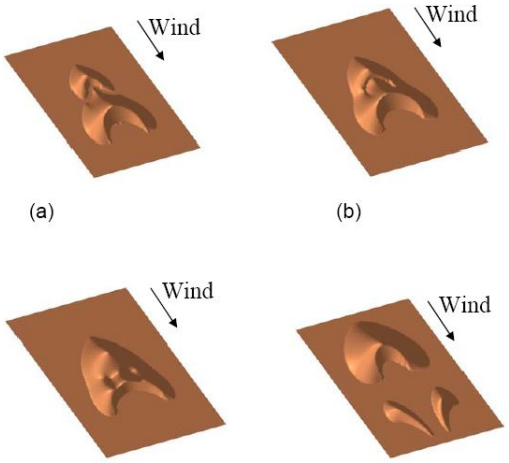

Figure 28: Simulation of barchans' breeding. The smaller dune bumps into the bigger one which leads to the birth of two baby dunes. Pictures happen in the alphabethical order.

In the intermediate hybrid state, the dune behind is not sufficiently fast-moving to wander all of the way up to the slip face of the bigger dune in front, because it gains so much sand that at some point it becomes larger, and therefore slower than the one in front. The dune that was previously bigger now becomes the smaller one, and its velocity becomes sufficiently large to leave the hybrid state. Effectively, it seems that the smaller dune crosses the bigger one, whereas in reality the two heaps never merge, owing to mass exchange. For some values of H and $\Delta H/h$, the emerging dune is larger than the incoming one; for some other values, it is smaller. This means that they do not behave exactly as solitons, but rather like solitary waves. For intermediate values of h and $\Delta H/h$ the two dunes exactly maintain their sizes and volumes that is, they behave like solitons. So for smaller $\Delta H/h$, we find two different situations (solitons and solitary waves). But if the height difference between the two dunes is very large, the small dune is entirely swallowed. And when height differences are moderate, we observe breeding respectively the creation of two baby dunes at

the horns of a barchan (see Figure 28).

Barchans are fundamentally unstable and do not necessarily behave like stable solitary waves. It was found that dune collisions and changes in wind direction destabilize the dunes and generate surface waves on the barchans . Because the resulting surface waves propagate at a higher speed than the dunes themselves (ten times faster according to observations), they can produce a series of new barchans of elementary size by breaking the horns of large dunes. The creation of these new dunes provides a mechanism for sand loss that prevents dune fields from merging into a single giant dune and therefore plays a fundamental role in the control of size selection and the development of dune patterns (see Figure 29).

Figure 29: A field of crescent-shaped barchan sand dunes in Peru. There can be seen surface waves on the barchans and a series of new barchanoids of elementary size reproduced by breaking the horns of large dunes.

4.2 Laboratory experiments

4.2.1 With aeolian barchan dunes

Because of the absence of dunes smaller than H=1m, W=19m and L=17.5m (for example see Figure 18) there were some attempts to generate an artificial dune from a small conical sandpile (10cm to 1m high) as shown on Figure 30.

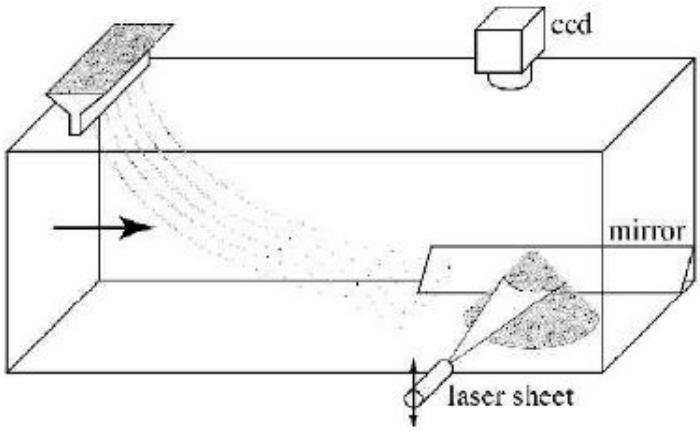

Figure 30: To study the time evolution of a sandpile blown by the wind, the Cemagref wind tunnel (6m long, 1mlarge, 1mhigh) was used. Pictures were taken from above by using a video camera. A mirror was placed at 45° to get on the same picture a side and a top view of the pile which was enlightened by a lamp and by a horizontal laser sheet adjustable in height which reveals the topography. A tunable sand supply has been add at the top of the tunnel. The grains were PVC beads of size $100\mu m$. The velocity (around 6m/s at 2cm above the soil covered by velvet) was chosen slightly above the threshold of grains' motion.

Time development of conical sandpile with (case b) and without (case a) sandsupply is represented on Figure 31. Nevertheless, the pile looses mass very quickly and disappears after a few minutes. So there exists a minimum size of barchans.

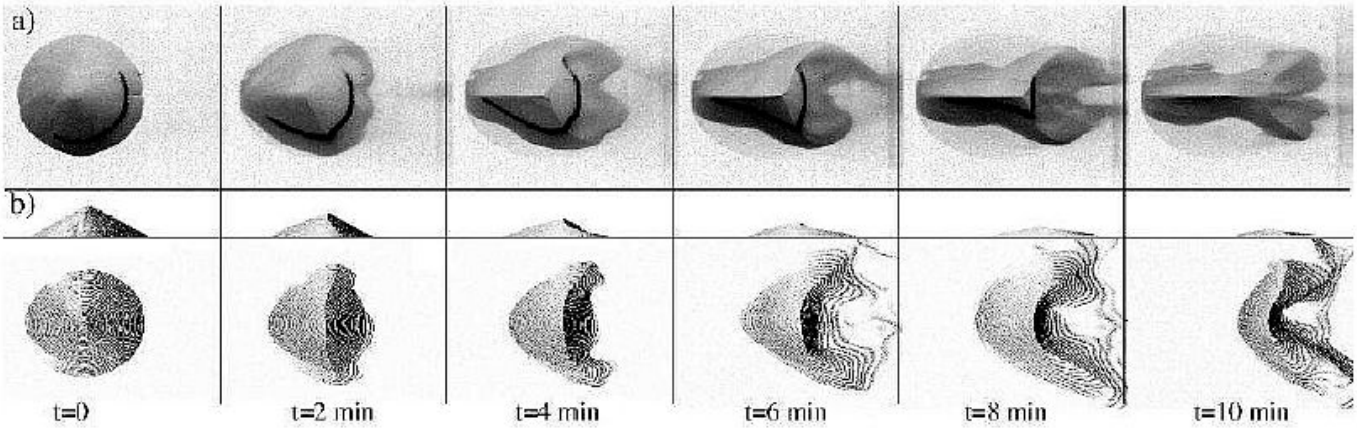

Figure 31: Time evolution of a sand pile blown out by a controlled wind without (a) and with (b) sand supply. In both cases the sandpile is eroded and disappears after a few minutes. Without sand supply, the erosion is localized on the sides so that a longitudinal brink is created. With a sand supply, the pile takes a crescent form: the back remains smooth and two horns grow by deposition of grains in reptation.

4.2.2 With subaqueous barchan dunes

If we want to reproduce barchans on a small scale than we have to reduce the typical length l_s: not with decreasing particle size (because of the cohesion that appears between grains below a certain size; typically $100\mu m$) but with increasing "atmospheric density" or better by using another driving fluid: water: so l_s becomes of the order of the grain diameter.

The experiment (see Figure 32) consists of a tray moving horizontally in a water tank. It is moved with a periodic and strongly asymmetric motion allowing to control the motion of the glass beads (grains with average diameter $150\mu m$) in only one direction (as seen in deserts). Typical amplitude and duration of the motion are 10cm and 1s for the initial movement and more than 2s for the way back.

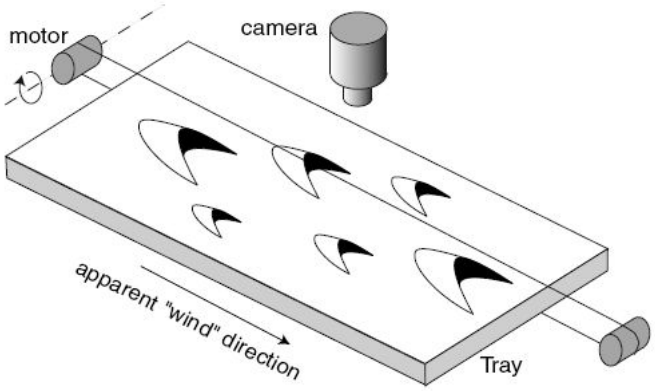

Figure 32: Experimental set-up. The tray (30cm by 15cm) is moved by a motor driven by a wave generator. A video camera is placed at the vertical of the tray to capture one image at each period of the motion.

The initial state, a homogenous grains layer, changed after a few hours (depends on the tray motion) into aquatic dune field (see Figure 33) where dunes propagate on the tray along the apparent wind direction.

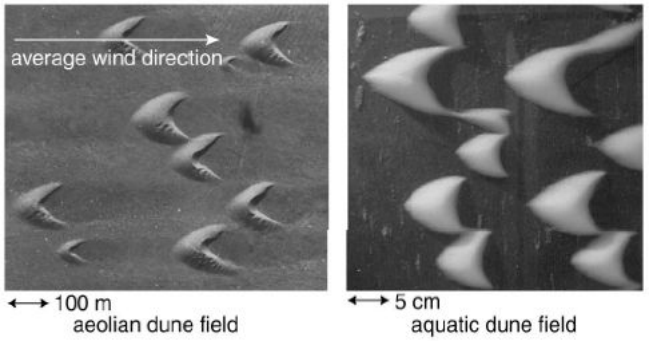

Figure 33: Aeolian and aquatic barchan field. The crescentic shape is quite similar in both cases.

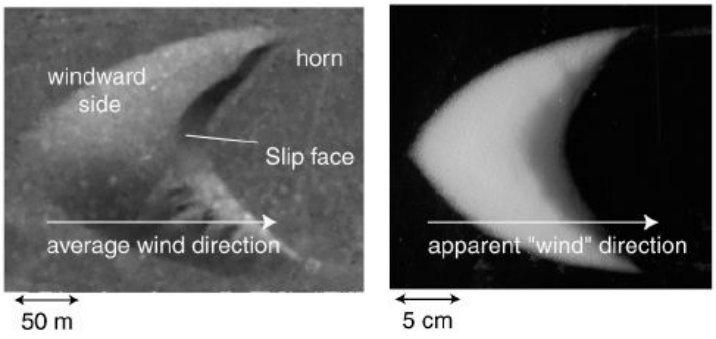

Figure 34: Real and artificial dunes. The left picture represents a typical aeolian barchan, the right one a typical aquatic.

So let me make a comparison between both types of dunes:

dune	typical length L	typical height H	
aquatic	1-10cm	1-10mm	depends on the initial amount of glass beads
aeolian	10-100m	1-10m	

Table 6: The comparison of barchan length and height for small and large dunes.

Obviously is there a factor around 1000 between the dimensions of these two kinds of dunes (see Figure 34). However, if we rescale measurements for both types of dunes by corresponding l_s we get pretty the same dependences of H(W) and L(W) as seen on Figure 35. That should be sufficient evidence that instead of measuring the aeolian dunes we can simply avoid all the obstacles by researching the aquatic dunes.

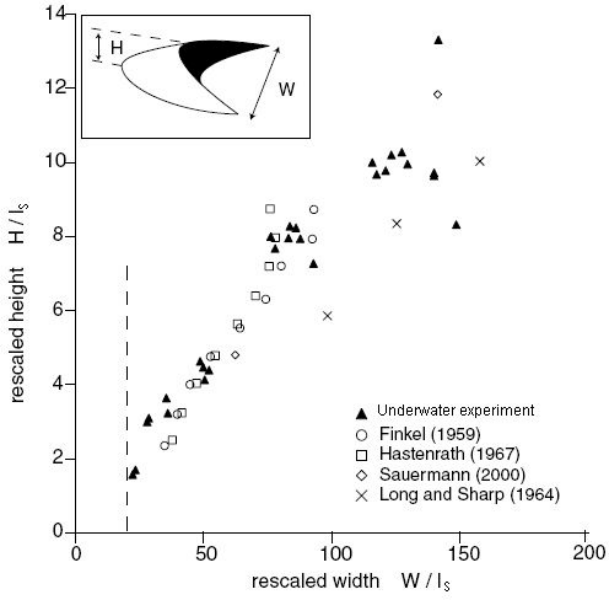

Figure 35: Experimental data for glass beads compared with field measurements, both rescaled by the corresponding l_s. The experiment presents a roughly linear relationship close to the field measurements. The existence of a minimal width of the order of 20 times l_s is pointed out by the dashed line: no dune smaller than this length appeared in the experiment nor in the field measurements.

5 Conclusion

In first two sections of this seminar I introduced dunes and barchans, in the third section I presented three models which go along with field measurements and laboratory experiments presented in section four pretty

well: minimal height and saturation length which were obtained from the models were proven in the field as well as in the lab. Not just that, in the field was also observed that dunes are not stable and when they lose their mass, they lose it from the horns which is in a good agreement wit C_C^C model.

There were lots of measurements already done and we still don't know everything. Even more for example typical measurements of the relationship between height and width or length lead to the assumption, that barchan dunes are shape invariant objects and on the other hand we have field measurements of entire dune shapes that have disproved this shape invariance. So there is huge amount of data that are contradictory. With other words there have to be even more measurements done to close open problems. Since the subaqueous barchans this shouldn't represent the obstacle as introduced in this seminar.

Contents

References

[1] K. Kroy, S. Fischer, B. Obermayer. *On the shape of barchan dunes*. cond-mat, 0501152, 2005.

[2] P. Hersen. *On the crescentic shape of barchan dunes*. Eur. Phys. J. B, 37:507514, 2004.

[3] R. A. Bagnold. *The Physics of Blown Sand and Desert Dunes*. Methuen, London, 1954.

[4] B. Andreotti, P. Claudin, S Douady. *Selection of dune shapes an velocities part 1: Dynamics of sand, wind and barchans*. Eur. Phys. J. B, (28):321-339, 2002.

[5] P. Hersen, S. Douady, B. Andreotti. *Relevant Length Scale of Barchan Dunes*. Phys. Rev. Lett., 89:264301, 2002.

[6] K. Kroy, X. Guo. *Comment on "Relevant Length Scale of Barchan Dunes"*. Phys. Rev. Lett., 93:039401, 2004.

[7] P. Hersen, K. H. Andersen, H. Elbelrhiti, B. Andreotti, P. Claudin, S. Douady. *Corridors of barchan dunes: Stability and size selection*. Phys. Rev. E, 69:011304, 2004.

[8] H. Elbelrhiti, P. Claudin, B. Andreotti. *Field evidence for surface-wave-induced instability of sand dunes*. Nature, 437:720723, 2005.

[9] V. Schwämmle, H. J. Herrmann. *Solitary wave behaviour of sand dunes*. Nature, 426:619620, 2003.

[10] D. R. Parsons, G. F. S. Wiggs, I. J. Walker, R. I. Ferguson, B. G. Garvey. *Numerical modeling of airflow over an idealized transverse dune*. Environmental Modelling & Software, 19:153162, 2004.

[11] H Momiji, R. Carretero-Gonzalez, S. R. Bishop, A. Warren. *Stimulation of the effect of wind speedup in the formation of transverse dune fields*. Earth Surf. Process. Landforms, 25:905918, 2000.

[12] S. E. Belcher, J. C. R. Hunt. *Turbulent flow over hills and waves*. Annu. Rev. Fluid Mech., 30:50738, 1998.

[13] G. Sauermann, K. Kroy, H. J. Herrmann. *Saturation Transients in Saltation and their Implications on Dune Shapes*. 2^{iem} Atelier International, Formation et Migration des Dunes, Nouakchott 7-13, 2001.

[14] D. Jerolmack, D. Mohrig. *Interactions between bed forms: Topography, turbulence and transport*. Journal of Geophy. Res., 110:F02014

[15] K. Kroy. *Minimal model for aeolian sand dunes*. Phys. Rev. E, 66:031302, 2002.

[16] K. Kroy, G. Sauermann, H. J. Herrmann. *Minimal Model for Sand Dunes*. Phys. Rev. Lett., 88:054301, 2002.

[17] G. Sauermann, K. Kroy, H. J. Herrmann. *A Continuum Saltation Model for Sand Dunes*. Phys. Rev. E, 64:031305, 2001.

[18] V. Schwämmle, H. J. Herrmann. *Modeling transverse dunes*. cond-mat, 0301589, 2003.

[19] P. Hersen, S. Douady, B. Andreotti. *Small Barchan Dunes in the Lab*. Geophy. Res., 5:01527, 2003.